SPE 80999

Effective and Ineffective Strategies for Mud Removal and Cement Slurry Design

I.A. Frigaard, SPE, University of British Columbia, and S. Pelipenko, Schlumberger

This paper was prepared for presentation at the SPE Latin American and Caribbean Petroleum Engineering Conference held in Port-of-Spain, Trinidad, West Indies, 27–30 April 2003.

Abstract

Uncontrolled flows of reservoir fluids behind the casing are relatively common. In worst cases these can lead to blow out, leakage at surface, destruction of subsurface ecology and potential freshwater contamination. Often, safe abandonment of such wells is not possible. A significant cause of flows behind the casing is ineffective mud removal during primary cementing.

The ideal situation is that drilling mud is displaced all around the annulus and that the displacement front advances steadily up the well at the pumping velocity. Even better is that the wide and narrow sides of the front advance at the same speed. Conversely, if the fluid on the narrow side of the annulus does not move, or moves very slowly, a longitudinal mud channel can result. Although the possibility of a narrow side mud channel and benefits of a steady state displacement have been recognised since the mid-1960s, there is still little quantitative understanding of when steady state displacements occur.

In this paper we present new results on the displacement of cementing fluids along eccentric annuli. We show that for certain combinations of the physical properties there will be a steady state displacement front. Furthermore, we are able to give an analytical expression for the shape of the front and indications of how the shape changes with the key physical parameters of the cementing process. These results are novel and have interesting implications for effective mud removal and complete zonal isolation during primary cementing.

Introduction

Primary cementing is a critically important operation in the construction of any oil well, (Ref. 1). Apart from providing structural integrity to the well, the chief purpose of the operation is to provide a continuous impermeable hydraulic seal in the annulus, preventing uncontrolled flow of reservoir fluids behind the casing. Serious problems may arise from such flows. Gas or oil may flow to surface causing a blowout, with consequent environmental damage and possible loss of life. Fluid migration into subsurface aquifers can cause contamination of drinking water, or can affect near-wellbore ecology. Even if surface casing vent flows are contained within the annulus, the fact of having pressure at surface prevents a well from being permanently abandoned, i.e. safely, at the end of its lifetime. Instead, these wells become permanently shut-in and remain an environmental risk. Financial consequences of poor zonal isolation on reservoir production are of course well known.

A widely cited industry figure, (Ref. 2), is that 15% of primary cementing jobs carried out in the US fail and that about 1/3 of these failures are due to gas or fluid migration. This problem exists worldwide, (e.g. about 9000 wells are suspended or temporarily abandoned in the U.S. Gulf Coast region). It is also particularly acute in Western Canada, where around 34,000 wells are currently shut-in and suspended, (Ref. 3), unable to be permanently abandoned due to gas pressures at surface, between the casing and formation, in the cement. Local variations in this problem can be extreme. For example, field survey results reported in Ref. 4, from Tangleflags, Wildmere and Abbey, (3 areas in Eastern Alberta), reveal that over a number of years, 0-12% (Tangleflags), 0-15% (Wildmere), and 80% (Abbey) of wells have been leaking in these regions.

One known cause of surface casing vent flows is that the cement, which is placed in the annulus between the outside of the casing and the inside of the hole, fails to fully displace the drilling mud that initially occupies this space. Incomplete mud removal can manifest in different ways. First, a coherent mud channel can form on the narrow side of the eccentric annulus. Second, residual mud or spacer can contaminate the cement as it sets. Third, mud may remain static in layers stuck to the inner and outer walls of the annulus. In the first or last case, the residual mud dehydrates as the cement sets and allows a porous conduit to develop in the annulus. In the case of severe contamination, the cement may not properly set.

These problems and the consequences described, provide the main motivation for this paper. This paper focuses on avoiding all three above cases, by ensuring that the initial displacement is steady. Unless there are significant losses during primary cementing, a steady stable displacement front advancing at the mean pumping speed all around the annulus is sufficient to ensure that the displacement is effective. Therefore, we consider the important question of whether these displacement fronts can be found in a realistic mathematical model of the process. Certainly, physical intuition tells us that certain simple cases should have steady displacement profiles, e.g. a heavy viscous fluid displacing a lighter less viscous fluid in a

concentric annulus. We show that this is the case and give analytical expressions for the shape of the steay displacement profiles. These analytical expressions indicate the variations with all process parameters and can be used for designing the rheology of cementing fluids.

Design methodologies for primary cementing that consider the rheology of the fluids have a long history. The possibility of a mud channel forming on the narrow side of the annulus was identified in Ref. 5. The reasoning used in Ref. 5 is essentially a hydraulic aproach. Extensions have led to systems of design rules for laminar displacements, (Refs. 6-10), based on hydraulic reasoning. In general, these rule sets state that the flow rate must be sufficiently high to avoid a mud channel on the narrow side of the annulus, that there should be a heirarchy of the fluid rheologies and that there should be a heirarchy of the fluid densities. Successful applications of such rule-based systems are given in Refs. 11-13 Whilst such approaches obviously contain a number of physical truths, the level of fundamental understanding is low and we can expect a reasonably high degree of conservatism in predictions made. A further problem with such systems is in making predictions for highly deviated and horizontal wellbores, since positive density differences, that help displacements in near vertical wells, tend to cause slumping towards the lower side of the annulus in highly deviated sections, see Refs. 14-16. In such wellbores, the focus must clearly be on rheology design.

More fundamental work has focused on computing the entire annular flow. However, this work is relatively recent. The first reliable analyses of narrow eccentric annular flows of visco-plastic fluids were carried out in the early 1990's, see Refs. 17-18, and this was only for flows of a single fluid and in 2 dimensions. Three-dimensional Newtonian displacements in eccentric annular geometries have been computed in Refs. 19-20, and CFD approaches have been followed in Ref. 21. However, these three-dimensional approaches are not particularly well-suited when it comes to designing displacements over the scale of the wellbore. This is partly because such software does not cope well with complex displacements, but also because the dimensions of the well, (i.e. very long), make uniform accuracy difficult to achieve.

A quite different approach involves averaging across the narrow annular gap, solving the resulting 2-dimensional model, see Refs. 22-26. This approach effectively models the annulus as an enorrmous eccentric annular Hele-Shaw cell. There is undoubtedly validity to this approach, due to the heirarchy of length-scales present in primary cementing geometries (i.e. axial length >> circumference >> annular gap). Indeed, in cases where the displacement of mud across the annular gap is complete, the approach in Refs 22-26 appears to be a rational way to model primary cementing displacements for design applications. It is this model that we follow here.

The Hele-Shaw approach that we follow does have the drawback of not addressing the possibility that mud may remain static in layers stuck to the inner and outer walls of the annulus, i.e. the so-called fluid-filled micro-annulus. These flows are extremely complex and are the subject of ongoing ivestigation, (Refs. 27-32).

Model Outline

We analyse the model derived in Refs 25-26, and here give only a brief overview of the model and its assumptions. Half of the annulus is considered and it is assumed that the flow is symmetric with the narrow side corresponding to the lower part of the annulus. Dimensionless spatial coordinates are (ϕ,ξ), where $0\le\phi\le 1$; $\phi=0$ denotes the wide side of the annulus, $\phi=1$ denotes the narrow side. The ξ-coordinate measures axial depth upwards from bottom-hole ($\xi=0$) to the top of the zone of interest, $\xi=Z$. The radial coordinate, across the annular gap, has been suppressed in the model derivation, by a combination of scaling arguments and averaging. Application of these methods is motivated by the fact that in a typical oil well the annular gap is much smaller than the annular circumference, which is much smaller than the axial length being cemented. The annular gap half-width is denoted $H(\phi,\xi)$, where to leading order:

$$H(\phi,\xi)=\overline{H}(\xi)\left[1+e(\xi)\cos\pi\phi\right] \qquad (1)$$

where $e(\xi)$ is the eccentricity at each axial depth, see Figure 1. The mean annular radius at each depth is denoted by $r_a(\xi)$ and the well inclination from vertical is $\beta(\xi)$. The flows considered are two-dimensional laminar flows, in which all flow variables have been averaged across the annular gap. The mass conservation equation is simply

$$\frac{1}{r_a}\frac{\partial}{\partial\phi}\left[H\overline{v}\right]+\frac{\partial}{\partial\xi}\left[H\overline{w}\right]=0 \qquad (2)$$

where $(\overline{v},\overline{w})$ are the averaged velocities in (ϕ,ξ)-directions, respectively. Equation (2) is satisfied by defining a stream-function Ψ:

$$\frac{1}{r_a}\frac{\partial\Psi}{\partial\phi}=H\overline{w},\qquad \frac{\partial\Psi}{\partial\xi}=-H\overline{v}. \qquad (3)$$

In terms of the stream function, the mean areal flow rate is $\left|\nabla_a\Psi\right|$, where

$$\nabla_a\Psi=\left(\frac{1}{r_a}\frac{\partial\Psi}{\partial\phi},\frac{\partial\Psi}{\partial\xi}\right). \qquad (4)$$

The model is essentially a Hele-Shaw model. In such a modeling approach it is found that the gap-averaged velocity field is parallel to the modified pressure gradient. The fluids are described by the Herschel-Bulkley model, with yield stress τ_Y, consistency κ and power law index n. The relationship between the mean speed and the magnitude of the modified pressure gradient, G, is found by considering a Poiseuille flow through a plane channel of separation $2H$. If the magnitude of the modified pressure gradient does not exceed a critical value, τ_Y/H, the fluid is unyielded at the walls and does not flow, $\left|\nabla_a\Psi\right|=0$. The excess of the pressure gradient over this critical value is denoted χ:

$$\chi=G-\frac{\tau_y}{H} \qquad (5)$$

The relationship between mean velocity and pressure drop is

derived in most texts on drilling fluid hydraulics. In terms of the areal flow rate, $|\nabla_a \Psi|$ and $\chi \geq 0$, this is:

$$|\nabla_a \Psi| = \frac{H^{m+2}}{\kappa^m (m+2)} \frac{\chi^{m+1}}{(\chi + \tau_y / H)^2} \left[\chi + \frac{(m+2)\tau_y}{(m+1)H} \right] \tag{6}$$

where $m = 1/n$. The function χ is only defined implicitly as a function of $|\nabla_a \Psi|$, and for an explict representation it is necessary to invert Eqn. 6 numerically, see Figure 2.

A sequence of fluids are pumped around the wellbore in a typical operation, but here we shall consider only what happens to the interface between two fluids, as the fluids are pumped along an annular section of constant eccentricity, inclination, mean gap width and mean radius. This simplification is not overly restrictive.

We consider only two fluids and divide the domain annular space (ϕ, ξ) into two regions. We let Ω_1 denote the lower displacing fluid (e.g. the spacer), and Ω_2 denote the upper displaced fluid (e.g. the mud). Following a similar procedure to that in Refs. 25-26, we can derive the following two equations for Ψ.

$$\begin{aligned} \nabla_{\mathbf{a}} \cdot \mathbf{S_1} &= 0 \qquad \text{in } \Omega_1 \\ \nabla_{\mathbf{a}} \cdot \mathbf{S}_2 &= 0 \qquad \text{in } \Omega_2 \end{aligned} \tag{7}$$

where for $k = 1,2$:

$$\begin{aligned} \mathbf{S_k} &= \left[\frac{\chi_k\left(|\nabla_a \Psi|\right) + \tau_{k,y} / H}{|\nabla_a \Psi|} \right] |\nabla_a \Psi| \quad \Leftrightarrow \quad |\mathbf{S_k}| > \tau_{k,y} / H \\ |\nabla_a \Psi| &= 0 \qquad\qquad\qquad\qquad\quad \Leftrightarrow \quad |\mathbf{S_k}| \leq \tau_{k,y} / H \end{aligned} \tag{8}$$

with χ_k derived from Eqn. 6, using the properties of fluid k.

We can see that Eqn. 7 is two nonlinear elliptic partial differential equations for Ψ.

The approach followed in Refs. 25-26 involves averaging across the narrow annular gap, to eliminate one dimension in the problem. This is effectively a Hele-Shaw approach. The fluids considered are visco-plastic, and the yield stress effect across the local channel width is reflected in the constitutive claosure laws (Eqn. 8). It is easy to see that $\mathbf{S_k}$ represents the modified pressure gradient in fluid k, and Eqn. 8 effectively says that the fluids will not flow locally in the narrow annulus unless a certain pressure gradient is exceeded, (sufficient for the fluid to yield). There is of course a direct analogy between Hele-Shaw flows and porous media flows. As such, the displacements in laminar primary cementing flows are very similar mathematically to a class of visco-plastic porous media flows studied in Refs. 33-34, by by Entov and co-workers. These visco-plastic models are often used to model reservoir flows of heavy oils.

Boundary conditions for Eqn. 7 on the wide and narrow side of the annulus are:

$$\Psi(0, \xi, t) = 0, \qquad \Psi(1, \xi, t) = Q(t), \tag{9}$$

where $Q(t)$ is the dimensionless flow rate. We assume that the interface is somewhere in the middle of the section of annulus being cemented and is denoted by $\xi = h(\phi, t)$. The interface evolves according to the kinematic condition:

$$\frac{\partial h}{\partial t} + \frac{\bar{v}}{r_a} \frac{\partial h}{\partial \phi} = \bar{w}\,. \tag{10}$$

Far away from the interface, we assume that Ψ becomes independent of ξ.

Two further conditions are needed to complete the model. These are the continuity of the stream function and the pressure, across the intereface. These conditions are given by:

$$\begin{aligned} &[\Psi]_1^2 = 0 \\ &\left[\frac{S_{k,\xi}}{r_a} + \frac{\rho_k \sin\beta \sin\pi\phi}{St} - \left(\frac{S_{k,\phi}}{r_a} + \frac{\rho_k \cos\beta}{St} \right) \frac{\partial h}{\partial \phi} \right]_1^2 = 0 \end{aligned} \tag{11}$$

where $[q]_1^2$ denotes the difference in a quantity q between fluid 2 and fluid 1 across the interface. The dimensionless densities of each fluid are denoted ρ_k, and St is the Stokes number, which represents the ratio of viscous to buoyancy forces in the flow. Note that the components of $\mathbf{S_k}$ may be expressed in terms of gradients of the stream function. This completes our model for laminar displacements. We have avoided deeper discussion about its derivation, since this may be found in Refs. 25-26.

Steady state displacements

The value of a steady state displacement has been discussed in the introduction. It is intuitive that such displacements can occur, but there is no quantitative guidance as to when they occur and how they vary with the process parameters. Here we show that it is possible to find an analytical expression that describes steady state solutions. We consider only a uniform section of annulus and suppose that the equations have been scaled according to the geometry of this section and the instantaneous flow rate. Then, we can assume that

$$\bar{H} = r_a = Q = 1\,, \tag{12}$$

and the mean dimensionless velocity in the displacement direction is equal to 1. Simply put, we ask if there is an interface solution that advances steadily at speed 1, i.e. such an interface would be stationary in a frame of reference that advances steadily up the well at the mean pumping velocity. We introduce a moving frame, $z = \xi - t$, denote the interface in this frame by $z = g(\phi, t) = h(\phi, t) - t$, and introduce the stream function in the moving frame, Φ, defined by:

$$\Psi = \Phi + \phi + \frac{e}{\pi} \sin\pi\phi \tag{13}$$

The kinematic equation is now:

$$(1 + e\cos\pi\phi)\frac{\partial g}{\partial t} - \frac{\partial \Phi}{\partial z}\frac{\partial g}{\partial \phi} = \frac{\partial \Phi}{\partial \phi} \tag{14}$$

and the boundary conditions are

$$\Phi(0, z, t) = 0 = \Phi(1, z, t)\,. \tag{15}$$

Thus, we see that if the interface is time-independent in the moving frame, it is also a streamline and additionally $\Phi(\phi, g(\phi)) = 0$ along a steady interface $z = g(\phi)$. We suppose that the steady state interface is centred at position $z = 0$, an a distance $\pm L$ away from the interface, we assume that the streamlines are parallel, and impose the condition:

$$\frac{\partial \Phi}{\partial z}(\phi, \pm L) = 0 . \qquad (16)$$

Finally, the jump conditions across the interface are:

$$\left[\Phi\right]_1^2 = 0$$

$$\left[\frac{\rho_k \sin\beta \sin\pi\phi}{St} - \frac{\rho_k \cos\beta}{St}\frac{\partial g}{\partial \phi}\right]_1^2 =$$

$$\left[\left(\frac{\chi_k + \tau_{k,Y} / (1 + e\cos\pi\phi)}{\left|\nabla(\Phi + \phi + (e/\pi)\sin\pi\phi)\right|}\right)\left(\frac{\partial \Phi}{\partial z} - \left(\frac{\partial \Phi}{\partial \phi} + 1 + e\cos\pi\phi\right)\frac{\partial g}{\partial \phi}\right)\right]_1^2 \qquad (17)$$

We use these to determine the interface shape.

Concentric annuli

This is certainly the simplest case possible, ($e = 0$), and one in which, at least when vertical, intuition tells us that there must be a steady state. If we set $\Phi = 0$, we see that both field Eqns. 7 are satisfied, as are all boundary conditions and the first jump condition. The pressure continuity condition Eqn. 17 remains to be satisfied, and this defines the interface shape, (up to an additive constant):

$$g(\phi) = -\frac{1}{\pi}\frac{b\sin\beta}{b\cos\beta + \left[\chi_k + \tau_{k,Y}\right]_1^2}\cos\pi\phi \qquad (18)$$

where b is a buoyancy parameter, defined by:

$$b = \frac{\rho_2 - \rho_1}{St} \qquad (19)$$

which will typically be negative since a more dense fluid is usually used to displace a lighter one. This solution leads to a number of insights.

(i) The term $\chi_k + \tau_{k,Y}$ is the modified pressure gradient in each fluid, which is in the axial direction only. Thus, the above fraction represents the ratio of differences in the azimuthal and axial modified pressure gradients. If the jump in modified pressure gradients is predominantly axial, the steady state will be quite flat, whereas if the jump is predominantly azimuthal the steady state will elongate along axis of the well. Thus, for a fixed density difference, increasing the frictional pressure drop in the displacing fluid, i.e. $\chi_1 + \tau_{1,Y}$, will tend to flatten the steady state profile.

(ii) Vertical wells: Here $\beta = 0$ giving the steady state $g(\phi) =$ constant , i.e. the interface is horizontal as expected.

(iii) Inclined well: With no rheology difference, we have simply

$$g(\phi) = -\frac{1}{\pi}\tan\beta\cos\pi\phi \qquad (20)$$

which implies that the interface aligns perpendicular to the direction of gravity. Note also that in primary cementing, the Stokes number is typically small, (e.g. $St \le 0.1$ would be common), so that relatively small density differences can lead to large buoyancy b. The above shape is that approached in the limit wen density effects are dominant, and is independent of the density difference.

(iv) Horizontal well: Here $\beta = \pi/2$ and we obtain:

$$g(\phi) = -\frac{1}{\pi}\frac{b\sin\beta}{\left[\chi_k + \tau_{k,Y}\right]_1^2}\cos\pi\phi \qquad (21)$$

In a horizontal well there will naturally be a tendency for the heavier fluid to slump towards the bottom of the annulus. Eqn. (21) is interesting in that it indicates that this potentially negative buoyancy effect can be compensated by proper design of the rheology difference between the fluids, resulting in a steady state.

Mildly eccentric annuli

In the case that the annulus is eccentric it is generally not possible to find an analytical expression for a steady state. In particular, as $e \to 1$ and the casing touches the wall of the well, it is clear that there can be no steady state. In general we might expect that there will be a critical eccentricity beyond which we are unable to find a steady state.

However, if we are very close to a concentric annulus, we also expect that we can find a solution that is somehow close to the concentric solution, Eqn. 18. We are in fact able to find this solution analytically, by using a perturbation method, in terms of the small parameter $e << 1$. The details of the derivation are rather involved, but may be found fully in Ref. 26. Here we just present the results of the analysis in Ref. 26.

To order e, the perturbed interface position is:

$$g(\phi) = -\frac{1}{\pi}\frac{b\sin\beta}{b\cos\beta + \left[\chi_k + \tau_{k,Y}\right]_1^2}\cos\pi\phi - \frac{e}{\pi^2}\frac{\sum_{k=1,2} P(\chi_k, \tau_{k,Y}, m_k)(\chi_k + \tau_{k,Y})\alpha_k \tanh\alpha_k L}{b\cos\beta + \left[\chi_k + \tau_{k,Y}\right]_1^2}\cos\pi\phi \qquad (22)$$

and the order e stream functions in the moving frame are:

$$\Phi(\phi, z) = eP(\chi_1, \tau_{1,Y}, m_1)\left(1 - \frac{\cosh\alpha_1(L+z)}{\cosh\alpha_1 L}\right)\frac{\sin\pi\phi}{\pi} \quad -L < z < 0$$

$$\Phi(\phi, z) = eP(\chi_2, \tau_{2,Y}, m_2)\left(1 - \frac{\cosh\alpha_2(L-z)}{\cosh\alpha_2 L}\right)\frac{\sin\pi\phi}{\pi} \quad 0 < z < L \qquad (23)$$

In the above the functions χ_k are evaualted at $\left|\nabla_a \Psi\right| = 1$ and $H = 1$. The function $P(\chi_k, \tau_{k,Y}, m_k)$ is strictly positive and is defined by:

$$P(\chi, \tau_Y, m) = \frac{(m+1)^2\chi^2 + (m+2)(2m+1)\chi\tau_Y + (m+1)(m+2)\tau_Y^2}{\chi\left[(m+1)\chi + (m+2)\tau_Y\right]} \qquad (24)$$

The parameter α_k is an eigenvalue of an intermediate

problem, and is given by:

$$\alpha_k^2 = \frac{\pi^2}{\chi_k + \tau_{k,Y}} \frac{\partial}{\partial |\nabla_a \Psi|} \chi_k , \qquad (25)$$

which must be evaluated numerically.

The solutions for the interface position, Eqn. 22, and for the stream function in each domain, Eqn. 23, are interesting primarily because all the problem parameters appear in the solutions, (eccentricity, inclination, density difference, fluid rheologies). Even though these solutions have been derived under the assumption that $e << 1$, the methodology does not necessarily break down immediately this condition is not satisfied. This is discussed further in Ref. 26.

In Eqn. 22 we can observe the effect of eccentricity on the concentric solution. The numerator of the 2nd term is strictly positive. Intuition tells us that the displacing fluid should be heavier and more viscous than the displaced fluid. In this case, the denominator of the second term is negative and we see that the 2nd term in Eqn. 22 is of form $eC\cos\pi\phi$, for some positive constant C. Thus, in a near vertical well, for positive density and frictional pressure differences, (as advocated for such field operations, e.g. see Ref. 9), the effect of eccentricity is to compensate for the first term in Eqn. 22, by extending the steady state interface upwards along the wide side.

Much of the algebraic complexity in our solutions is due to the fluids having a yield stress. When there is no yield stress present, explict formulas can be derived for most of the parameters. Equations 22-23 become:

$$g(\phi) = -\frac{1}{\pi} \frac{b \sin\beta}{b\cos\beta + \left[\kappa_k (m_k+1)^{1/m_k}\right]_1^2} \cos\pi\phi - \frac{e}{\pi^2} \frac{\sum_{k=1,2} \kappa_k (m_k+1)^{1+1/m_k} m_k^{-1/2} \tanh\left(\pi m_k^{-1/2} L\right)}{b\cos\beta + \left[\kappa_k (m_k+1)^{1/m_k}\right]_1^2} \cos\pi\phi \qquad (26)$$

and the order e stream functions in the moving frame are:

$$\Phi(\phi, z) = e(m_1+1)\left(1 - \frac{\cosh \pi m_1^{-1/2}(L+z)}{\cosh \pi m_1^{-1/2} L}\right)\frac{\sin\pi\phi}{\pi} \qquad -L < z < 0$$

$$\Phi(\phi, z) = e(m_2+1)\left(1 - \frac{\cosh \pi m_2^{-1/2}(L-z)}{\cosh \pi m_2^{-1/2} L}\right)\frac{\sin\pi\phi}{\pi} \qquad 0 < z < L \qquad (27)$$

Numerical Examples

It is of interest to explore the parametric variations in our results. The results are valid for a mildly eccentric uniform narrow annulus. In order to reinterpret the dimensionless results in terms of dimensional variables, it is necessary to scale the variables. We denote the dimensional outer & inner radii and the flow rate, by $\hat{R}_o, \hat{R}_i, \hat{Q}$, respectively, (the hat symbol being used to denote a dimensional quantity). The dimensional rheological parameters for fluid k are: $\hat{\tau}_{k,Y}$, $\hat{\kappa}_k$, n_k, $\hat{\rho}_k$, the yield stress, consistency, power law index and density respectively. The gravitational acceleration is denoted $\hat{g}$. With these definitions, the scales we have employed are:

$$\text{Length-scale} = \frac{\pi}{2}\left(\hat{R}_o + \hat{R}_i\right)$$

$$\text{Annular halfgap-scale} = \frac{1}{2}\left(\hat{R}_o - \hat{R}_i\right)$$

$$\text{Stream-function scale} = \frac{\hat{Q}}{4}$$

$$\text{Velocity scale} = \frac{\hat{Q}}{\pi\left[\hat{R}_o^2 - \hat{R}_i^2\right]} = \hat{w}^*$$

$$\text{Shear rate scale} = \frac{\hat{w}^*}{\frac{1}{2}\left[\hat{R}_o - \hat{R}_i\right]} = \hat{\dot{\gamma}}^*$$

$$\text{Stress scale} = \max_{k=1,2}\left\{\hat{\kappa}_k \left(\hat{\dot{\gamma}}^*\right)^{n_k} + \hat{\tau}_{k,Y}\right\} = \hat{\tau}^*$$

$$\text{Viscosity scale} = \frac{\hat{\tau}^*}{\hat{\dot{\gamma}}^*} = \hat{\mu}^*$$

$$\text{Density scale} = \max_{k=1,2}\left\{\hat{\rho}_k\right\} = \hat{\rho}^*$$

$$\text{Stokes number, } St = \frac{\hat{\tau}^*}{\hat{\rho}^* \hat{g} \frac{1}{2}\left[\hat{R}_o - \hat{R}_i\right]} \qquad (28)$$

Stream function and flow near the interface

In Figures 3-5 we plot 3 examples of the stream function solution, in the moving frame, Eqn. 23. It is interesting to observe that these stream function solutions are independent of buoyancy and inclination to leading order. Thus, the flux of fluid from the narrow side to the wide side depends primarily on the rheological differences. In Figure 3 the displacing fluid has significantly higher yield stress, consistency and power law index than the displaced fluid. It is noticeable that the streamlines are more densely packed in the less viscous upper fluid, indicating that effects of eccentricity are felt more acutely there. Figure 4 preserves the same rheology, but reduces the eccentricity. The reduction in the stream function is linear with the eccentricity. In Figure 5 we increase the yield stress, consistency and power law index of the displaced fluid, to something close to that of fluid 1. The streamlines in the two domains are quite similar.

A key point to note is that the flows in the two domains are moving counter-current to one-another at the interface. As is common in a Hele-Shaw type model, the normal component of velocity is continuous across the interface, but not the tangential component. We must assume that if the counter-current interfacial flow becomes too strong, the shear flow will destabilize the effects of gravity and we will have some form of local mixing. This type of instability is likely to be of Kelvin-Helmoltz type, but has not been studied in this context.

In Figures 3-5 it is noted that the domains of the 2 fluids are rectangular, since the interface perturbation is assumed to be of order $e << 1$, and this has been lnearised. Buoyancy and inclination will affect the interface shape significantly (see below). It is believed that they will also enter into the stability problem. In a similar context, interfacial shear instabilities

have been observed in a series of experiments, reported in Ref. 23, notably where the narrow side interface forms a long tail.

Steady state shape

In Figures 6-11 we explore the variations in steady state interface shape with the different model parameters. Our method is to fix a base case of model parameters: $\beta = 0.1$, $e = 0.05$, $b = -1$, $\tau_{1,Y} = 1$, $\kappa_1 = 1$, $m_1 = 1$, $\tau_{2,Y} = 0.8$, $\kappa_2 = 0.8$, $m_2 = 1.0$, and then to vary each parameter in turn. The solution $g(\phi)$ in Eqn. 22 is the sum of the concentric solution Eqn. 18 and a term multiplied by the eccentricity. We denote these two contributions by $g_{conc}(\phi)$ & $g_{ecc}(\phi)$ respectively, i.e.

$$g(\phi) = g_{conc}(\phi) + g_{ecc}(\phi). \qquad (29)$$

In Figures 6-11 we plot each of: $g(\phi)$, $g_{conc}(\phi)$ & $g_{ecc}(\phi)$, for the different parametric variations. This enables us to see the competition between the concentric solution and the effect of eccentricity. In some cases a parameter change affects the two solutions in opposite directions, reducing the net effect. Our model has assumed also that the concentric solution is also of order e, which means that changes in $g_{conc}(\phi)$ are often smaller than changes in $g_{ecc}(\phi)$.

The principal results can be summarised as follows.

(i) $g_{conc}(\phi)$ is elongated in the negative direction, (meaning the wide side interface is below the narrow side interface and the absolute separation between wide and narrow side increases), by the following variations: increasing β, $\tau_{2,Y}$ κ_2 $n_2 = 1/m_2$; decreasing, b, $\tau_{1,Y}$, κ_1, $n_1 = 1/m_1$. Changes in the eccentricity, e, leave $g_{conc}(\phi)$ unaffected.

(ii) $g_{ecc}(\phi)$ is elongated positively, (meaning the wide side interface is above the narrow side interface and the absolute separation between wide and narrow side increases), by the following variations: increasing β, b, e, $\tau_{2,Y}$ κ_2 $n_2 = 1/m_2$; decreasing $\tau_{1,Y}$, κ_1, $n_1 = 1/m_1$.

In making the above statements, we have explored only small parametric variations about a set of parameters that might be thought sensible to achieve a stable steady state displacement, i.e. we have chosen a hierarchy in both the rheological parameters and in the densities of the 2 fluids, (heavy & viscous displaces light & less viscous). In this case the quantity

$$b\cos\beta + \left[\chi_k + \tau_{k,Y}\right]_1^2, \qquad (30)$$

which appears in the denominator of the two terms in Eqn 22, will typically be negative. If we instead consider fluids for which the above term becomes zero, or is positive, it is evident that the solutions can become singular, e.g. if we consider a negative rheology difference versus a positive density difference. Many of these solutions are intuitively unstable, some are mechanically unstable and others are known to be vulnerable to viscous fingering-type instabilities. These solutions have therefore not been explored here.

Conclusions

This paper has addressed the issue of whether steady state displacements can exist during primary cementing of an oil well. Steady state solutions have been presented, discussed and explored in some depth. These analytical solutions serve a number of important purposes:

1. They confirm unequivocally that steady state displacements can exist in primary cementing.
2. They allow quick comparison with our physical intuition. In particular this is true for the concentric annular solutions.
3. The solutions give a direct quantitative indication of how large competing effects of different parameters are, at least within the range of validity. For example, one might estimate the rheology difference required to counter slumping effects in a horizontal displacement.
4. The solutions provide a test case for numerical solutions.

Despite of the usefulness of these expressions, the results are in a sense incomplete in that we have not considered the question of stability. For example, it is evident in Eqn. 18 that if we interchange the fluid properties between fluids 1 and 2, we will leave the shape of steady state unchanged! Similar effects can be achieved in playing with the eccentric annular solution. Certainly, some of these configurations (e.g. a light fluid displacing a heavy fluid, with identical rheology) are simply mechanically unstable, and would not be observed in reality. The question of whether there exist stable steady states is harder to answer, and is a topic for further study. We mention that numerical results shown in Ref. 25 do suggest that stable steady states are found in practice, for certain parameter combinations.

In terms of testing a cement job design, one could first check that the shape of the steady state prediced via Eqn. 22 is not mechanically unstable, and then run a simple simulation, e.g. using the computer simulaion in Ref. 25, to investigate its stability. In preference, one would also want to displace with a wide-side vs narrow side separation that is not too large, and for this the results in Eqn. 22, illustrated in Figures 6-11, give a good indication of how to design the rheology to achieve this. However, in order of priority, a stable displacing interface must take priority over ensuring a small separation.

In the situation of a vertical concentric annulus, it might be possible to improve one's understanding of stability via analytical methods. This situation corresponds to a planar displacement along the axis of the annulus. Similarly, an approximately planar displacement can be achieved for certain solutions with small eccentricity, i.e. where $g_{conc}(\phi)$ & $g_{ecc}(\phi)$, approximately balance each other. Local stability analyses of this type of flow have been carried out in Refs. 35-37, in the context of a porous media displacement of non-Newtonian fluids. The stability of planar displacement of a Herschel-Bulkley fluid in a Hele-Shaw cell, (i.e.~the Saffman-Taylor problem), has been partly addressed in Refs. 38-40. Thus, the techniques exist to address this problem, and it is simply a question of adaptation.

Although such stability studies are partly relevant, it must be noted that this type of analysis will be local and is focused at instability, meaning avoiding local viscous fingering of the interface. If such instabilities do start, a more relevant question is whether they grow indefinitely or whther there is some sort of nonlinear saturation. Also, as we have discussed, there

exists the possibility for shear instabilities at the interface, since the secondary flow is counter-current. Again, the real question here is whether these instabilities grow or saturate. In the context of primary cementing of a well, which is extremely long compared to the circumferential distance, it is only the global behaviour of an instability that can be of concern. If there is some local mixing or small separation of the front, it becomes irrelevant over the scale of the well and is unlikely to compromise the hydraulic isolation of the cement job. In a subsequent paper we will address the important question of prediction of such global defects.

Acknowledgements

This research has been carried out at the University of British Columbia, supported financially by Schlumberger and NSERC, through CRD project 245434, as well as by the Pacific Institute for the Mathematical Sciences. This support is gratefully acknowledged.

References

1. E.B. Nelson, *Well Cementing*. Schlumberger Educational Services, (1990).
2. K. Newman, *Cement pulsation improves gas well cementing*. World Oil, July 2001, 89-94.
3. B. Nichol, *Choosing Economic Options for Shut-in Wells with a Risk Assessment Approach*. Presentation at: Cost-effective Abandonment Solutions, Technology Information Session, Calgary May 3, 2000. Meeting organised by PTAC (Petroleum Technology Alliance Canada).
4. D. Dustrehoft, G. Wilson and K. Newman, *Field Study on the Use of Cement Pulsation to Control Gas Migration*. Society of Petroleum Engineers paper number SPE 75689 (2002).
5. R.H. McLean, C.W. Manry and W.W. Whitaker, *Displacement Mechanics in Primary Cementing*. Society of Petroleum Engineers paper number SPE 1488, (1966).
6. A. Jamot, *Deplacement de la boue par le latier de ciment dans l'espace annulaire tubage-paroi d'un puits*. Revue Assoc. Franc. Techn. Petr., **224**, pp. 27-37, (1974).
7. C.F. Lockyear and A.P. Hibbert, *Integrated Primary Cementing Study Defines Key Factors for Field Success.* Journal of Petroleum Technology, December 1989, pp. 1320-1325.
8. C.F. Lockyear, D.F. Ryan and M.M. Gunningham, *Cement Channelling: How to Predict and Prevent.* Society of Petroleum Engineers paper number SPE 19865, (1989).
9. D. Guillot, H. Hendriks, F. Callet and B. Vidick, *Mud Removal.* Chapter 5 in *Well Cementing.* editor E.B. Nelson, Schlumberger Educational Services, Houston, (1990).
10. M. Couturier, D. Guillot, H. Hendriks and F. Callet, *Design Rules and Associated Spacer Properties for Optimal Mud Removal in Eccentric Annuli.* Society of Petroleum Engineers, paper number SPE 21594, (1990).
11. S. Brady, P.P. Drecq, K.C. Baker and D.J. Guillot, *Recent Technological Advances Help Solve Cement Placement Problems in the Gulf of Mexico.* Society of Petroleum Engineers paper IADC/SPE 23927, (1992).
12. D.F. Ryan, D.S. Kellingray and C.F. Lockyear, *Improved Cement Placement on North Sea Wells Using a Cement Placement Simulator.* Society of Petroleum Engineers paper number SPE 24977, (1992).
13. V.C. Kelessidis, R. Rafferty, A. Merlo and R. Maglione, *Simulator Models U-tubing to improve primary cementing.* Oil and Gas Journal, March 7th 1994, pp. 72-80.
14. S.R. Keller, R.J. Crook, R.C. Haut and D.S. Kulakofsky, *Deviated-Wellbore Cementing: Part 1 - Problems.* Journal of Petroleum Technology, August 1987, pp. 955-960.
15. R.J. Crook, S.R. Keller, and M.A. Wilson, *Deviated Wellbore Cementing: Part 2 - Solutions.* Journal of Petroleum Technology, August 1987, pp. 961-966.
16. F.L. Sabins, *Problems in Cementing Horizontal Wells.* Journal of Petroleum Technology, April 1990, pp. 398-400.
17. I.C. Walton and S.H. Bittleston, *The axial flow of a Bingham Plastic in a narrow eccentric annulus*, J. Fluid Mech., **222**, pp. 39-60, (1991).
18. P. Szabo and O. Hassager, *Flow of viscoplastic fluids in eccentric annular geometries.* J. Non-Newtonian Fluid Mech., **45**, pp. 149-169, (1992).
19. P. Szabo and O. Hassager, *Simulation of Free Surfaces in 3-D with the Arbitrary Lagrange-Euler Method.* Int. J. Num Methods in Eng., **38**, pp. 717-734, (1995).
20. P. Szabo and O. Hassager, *Displacement of One Newtonian Fluid by Another: Density Effects in Axial Annular Flow*. Int. J. Multiphase Flow, **23**(1), pp. 113-129, (1997).
21. N. Barton, G.L. Archer & D.A. Seymour, *Computational fluid dynamics improves liner cementing operation*. Oil & Gas Journal, September 26, pp. 92-98, (1994)
22. M. Martin, M. Latil and P. Vetter, *Mud Displacement by Slurry during Primary Cementing Jobs - Predicting Optimum Conditions.* Society of Petroleum Engineers paper number SPE 7590, (1978).
23. A. Tehrani, S.H. Bittleston and P.J.G. Long, *Flow instabilities during annular displacement of one non-Newtonian fluid by another.* Experiments in Fluids 14, pp. 246-256, (1993).
24. A. Tehrani, J. Ferguson and S.H. Bittleston, *Laminar Displacement in Annuli: A Combined Experimental and Theoretical Study.* Society of Petroleum Engineers paper number SPE 24569, (1992).
25. S.H. Bittleston, J. Ferguson & I.A. Frigaard, *Mud removal and cement placement during primary cementing of an oil well*. J. Engng. Math., 43, pp. 229-253, (2002).
26. S. Pelipenko & I.A. Frigaard, On steady state displacements in primary cementing of an oil well. Submitted to J. Engng. Math., August (2002).
27. C. Gabard, Etude de la stabilité de films liquides sur les parois d'une conduite verticale lors de l'ecoulement de fluides miscibles non-newtoniens. These de l'Universite Pierre et Marie Curie (PhD thesis), Orsay, France, 2001.
28. M. Allouche, I.A. Frigaard, and G. Sona, Static wall layers in *the displacement of two visco-plastic fluids in a plane channel.* J. Fluid Mech., 424, pp. 243-277, (2000).
29. I.A. Frigaard, O. Scherzer and G.Sona, *Uniqueness and non-uniqueness in the steady displacement of two viscoplastic fluids.* ZAMM, 81(2), pp. 99-118, (2001).
30. I.A. Frigaard, M. Allouche & C. Gabard, *Incomplete Displacement of Viscoplastic Fluids in Slots and Pipes-Implications for Zonal Isolation.* Society of Petroleum Engineers paper number: SPE 64998, February (2001).
31. I.A. Frigaard, M. Allouche & C. Gabard, *Setting rheological targets for chemical solutions in mud removal and cement slurry design*. Journal of Petroleum Technology, August (2001).
32. I.A.Frigaard, S. Leimgruber & O. Scherzer, *Variational methods and maximal residual wall layers.* Submitted to J. Fluid Mechanics, March 2002.
33. G.I. Barenblatt, V.M. Entov & V.M. Ryzhik, *Theory of fluid flows through natural rocks*. Theory and Applications of Transport in Porous Media, volume 3. Kluwer (1990).

34. R.V. Goldstein & V.M. Entov, *Qualitative Methods in Continuum Mechanics*, Wiley, New York, (1994).
35. H. Pascal, *Rheological behaviour effect of non-Newtonian fluids on dynamic of moving interface in porous media*. Int. J. Engng. Sci. 22(3) pp. 227-241, (1984).
36. H. Pascal, *Dynamics of moving interface in porous media for power law fluids with a yield stress*. Int. J. Engng. Sci. 22(5) pp. 577-590 (1984).
37. H. Pascal, *A theoretical analysis of stability of a moving interface in a porous medium for Bingham displacing fluids and its application in oil displacement mechanism*. Can. J. Chem. Engng. 64 pp. 375-379, (1986).
38. S.D.R.~Wilson, *The Taylor-Saffman problem for a non-Newtonian liquid*. J. Fluid Mech. 220, pp. 413-425, (1990).
39. V.A. Gorodtsov and V.M. Yentov, *Instability of the displacement fronts of non-Newtonian fluids in a Hele-Shaw cell*. J. Appl. Maths Mechs. 61, pp. 111-126, (1997).
40. P. Coussot, Saffman-Taylor instability in yield-stress fluids. J. Fluid Mech. 380, pp. 363-376, (1999).

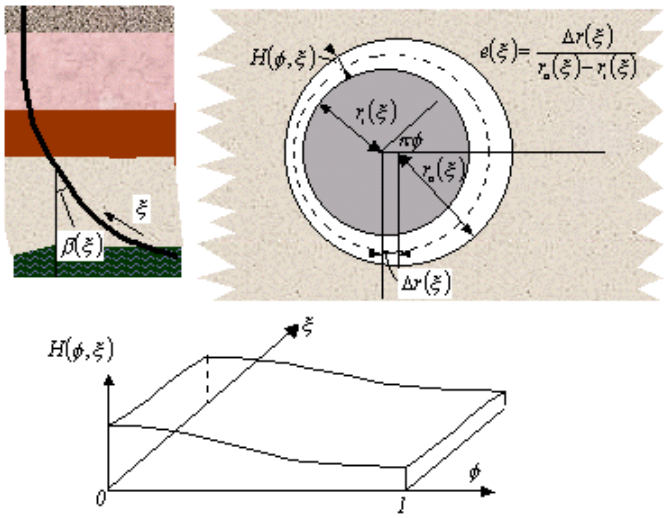

Figure 1. Schematic of the model geometry

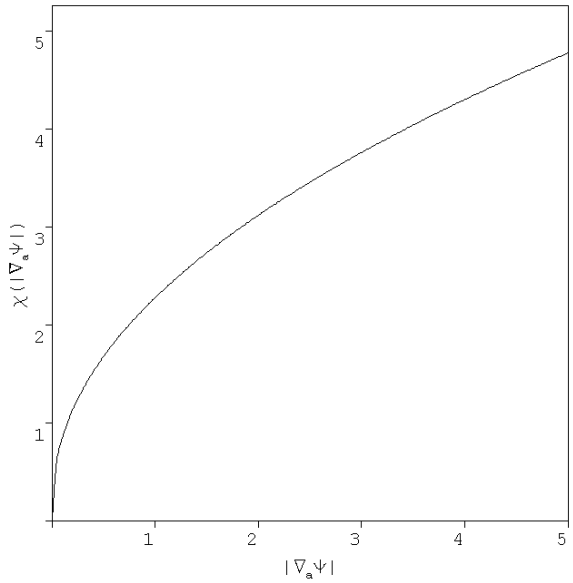

Figure 2. The nonlinear function $\chi\left(\left|\nabla_a\Psi\right|\right)$, for parameters: $\tau_Y=\kappa=H=1$, $m=2$.

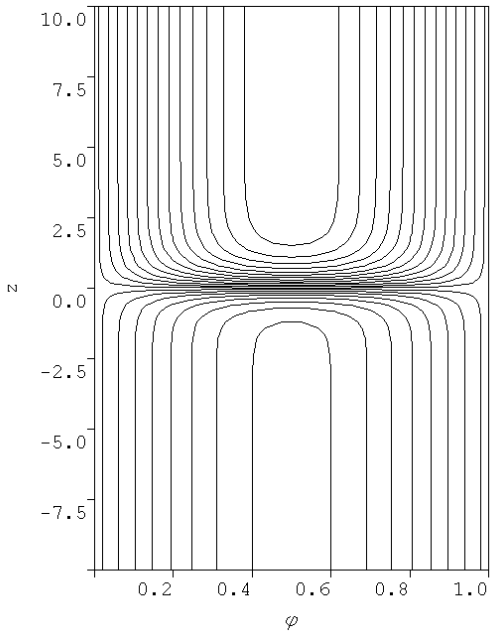

Figure 3. The function Φ, for parameters: $e=0.1$, $L=10$, $\tau_{1,Y}=\kappa_1=m_1=1$, $\tau_{2,Y}=0.5, \kappa_2=0.5, m_2=2$. Streamlines are spaced at intervals $\Delta\Phi=0.01$.

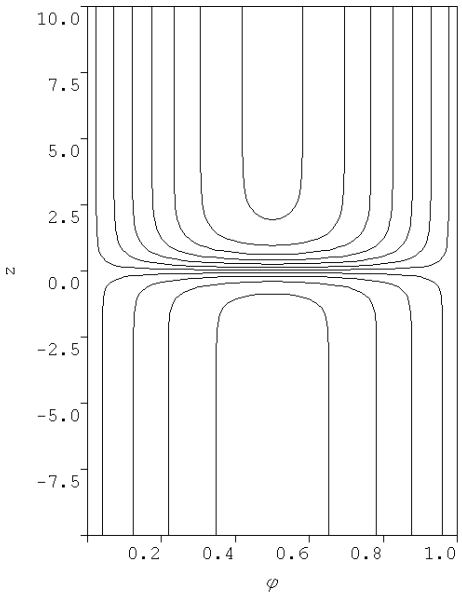

Figure 4. The function Φ, for parameters: $e=0.05$, $L=10$, $\tau_{1,Y}=\kappa_1=m_1=1$, $\tau_{2,Y}=0.5, \kappa_2=0.5, m_2=2$. Streamlines are spaced at intervals $\Delta\Phi=0.01$.

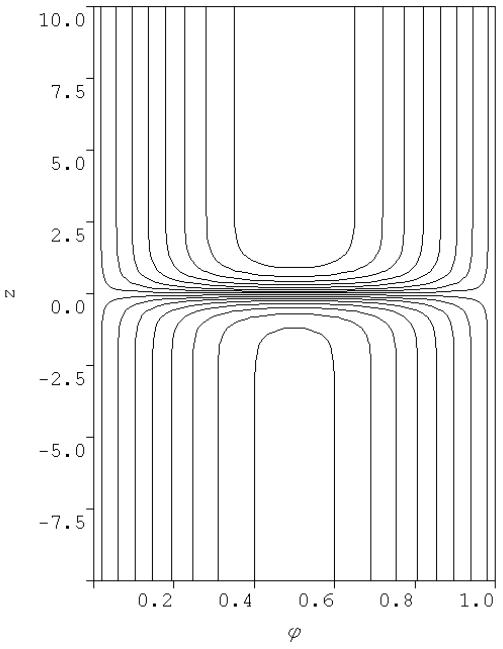

Figure 5. The function Φ, for parameters: $e = 0.1$, $L = 10$, $\tau_{1,Y} = \kappa_1 = m_1 = 1$, $\tau_{2,Y} = 0.9, \kappa_2 = 0.9, m_2 = 1.1$. Streamlines are spaced at intervals $\Delta\Phi = 0.01$.

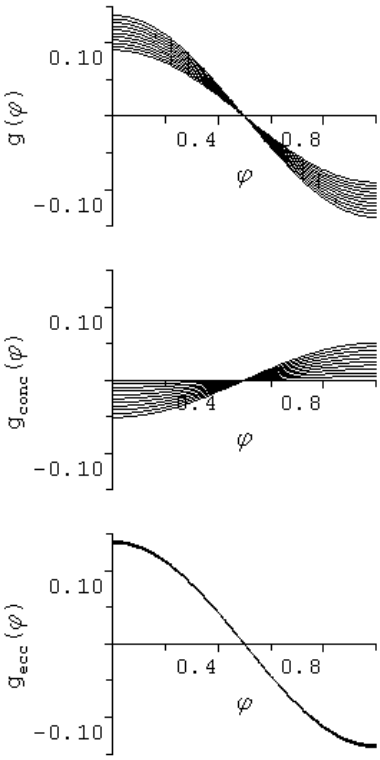

Figure 6. Parametric variations in $g(\phi)$, $g_{conc}(\phi)$ & $g_{ecc}(\phi)$ with inclination β: $\beta = 0.0, 0.03, 0.06, \cdots, 0.3$; $g_{conc}(\phi)$ elongates negatively, $g_{ecc}(\phi)$ elongates positively. Fixed parameters are: $e = 0.05$, $b = -1$, $\tau_{1,Y} = 1$, $\kappa_1 = 1$, $m_1 = 1$, $\tau_{2,Y} = 0.8$, $\kappa_2 = 0.8$, $m_2 = 1.0$.

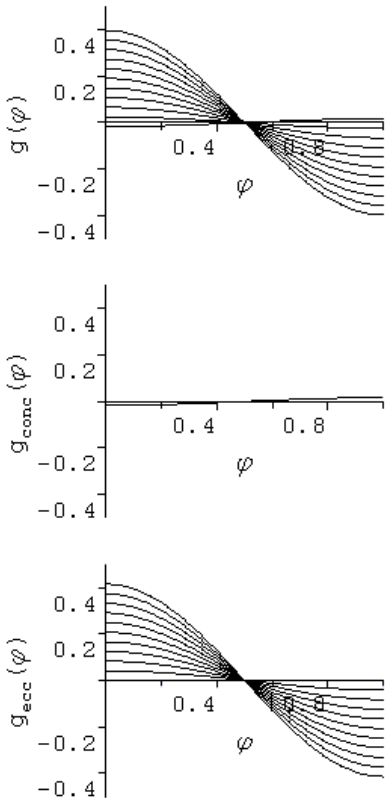

Figure 7. Parametric variations in $g(\phi)$, $g_{conc}(\phi)$ & $g_{ecc}(\phi)$ with eccentricity, e: $e = 0.0, 0.015, 0.03, \cdots, 0.15$; $g_{conc}(\phi)$ is unaffected, $g_{ecc}(\phi)$ elongates positively. Fixed parameters are: $\beta = 0.1$, $b = -1$, $\tau_{1,Y} = 1$, $\kappa_1 = 1$, $m_1 = 1$, $\tau_{2,Y} = 0.8$, $\kappa_2 = 0.8$, $m_2 = 1.0$.

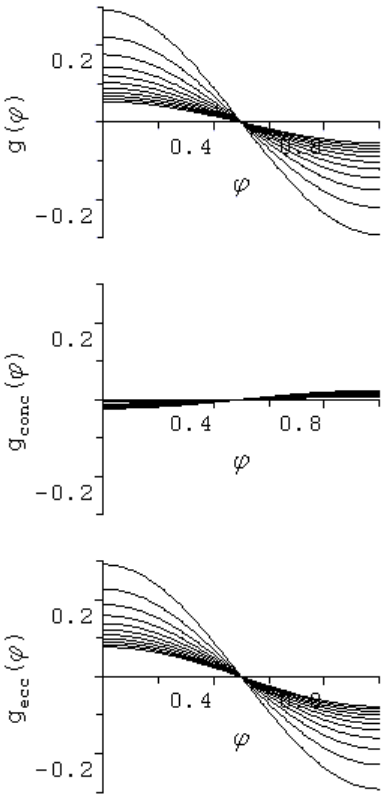

Figure 8. Parametric variations in $g(\phi)$, $g_{conc}(\phi)$ & $g_{ecc}(\phi)$ with buoyancy: $b = 0.0, -0.25, -0.5, \cdots, -2.5$; $g_{conc}(\phi)$ elongates negatively, $g_{ecc}(\phi)$ flattens. Fixed parameters: $\beta = 0.1$, $e = 0.05$, $\tau_{1,Y} = 1$, $\kappa_1 = 1$, $m_1 = 1$, $\tau_{2,Y} = 0.8$, $\kappa_2 = 0.8$, $m_2 = 1.0$.

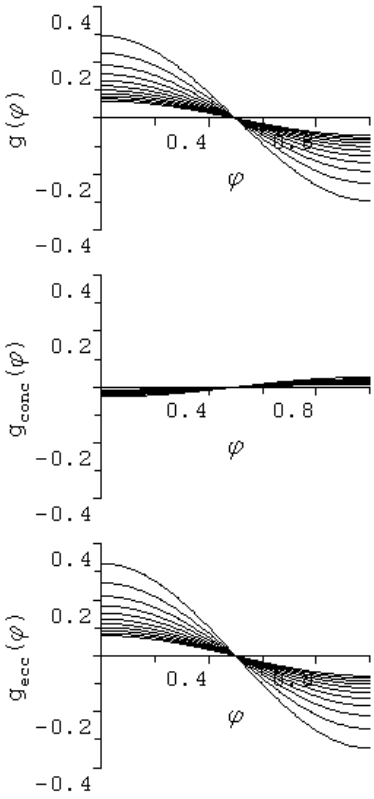

Figure 9. Parametric variations in $g(\phi)$, $g_{conc}(\phi)$ & $g_{ecc}(\phi)$ with displaced fluid yield stress $\tau_{2,Y}$: $\tau_{2,Y} = 0.0, 0.15, 0.3, \cdots, 1.5$; $g_{conc}(\phi)$ elongates negatively, $g_{ecc}(\phi)$ elongates positively. Fixed parameters: $\beta = 0.1$, $e = 0.05$, $b = -1$, $\tau_{1,Y} = 1$, $\kappa_1 = 1$, $m_1 = 1$, $\kappa_2 = 0.8$, $m_2 = 1.0$.

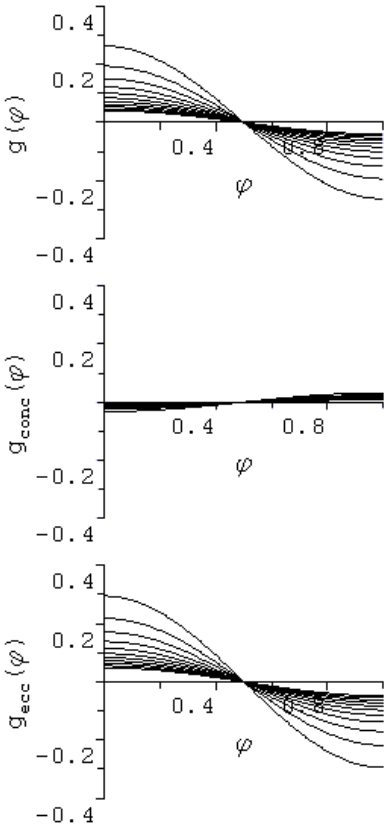

Figure 10. Parametric variations in $g(\phi)$, $g_{conc}(\phi)$ & $g_{ecc}(\phi)$ with displaced fluid consistency κ_2: $\kappa_2 = 0.1, 0.2, 0.3, \cdots, 1.1$; $g_{conc}(\phi)$ elongates negatively, $g_{ecc}(\phi)$ elongates positively. Fixed parameters: $\beta = 0.1$, $e = 0.05$, $b = -1$, $\tau_{1,Y} = 1$, $\kappa_1 = 1$, $m_1 = 1$, $\tau_{2,Y} = 0.8$, , $m_2 = 1.0$.

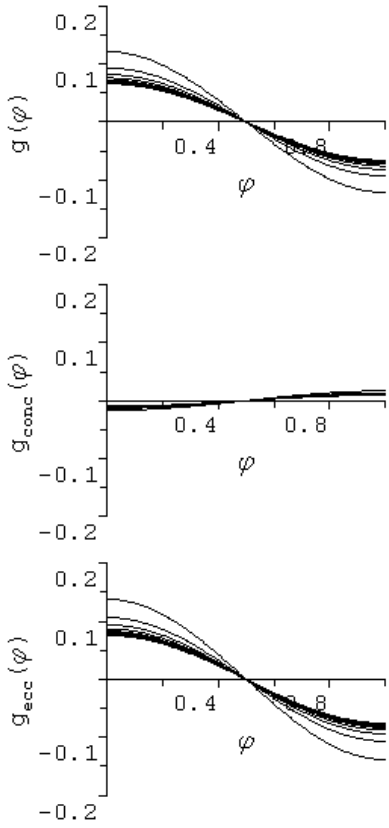

Figure 11. Parametric variations in $g(\phi)$, $g_{conc}(\phi)$ & $g_{ecc}(\phi)$ with displaced fluid inverse power law index m_2: $m_2 = 1.0, 1.3, 1.6, \cdots, 4.0$; $g_{conc}(\phi)$ flattens, $g_{ecc}(\phi)$ flattens. Fixed parameters: $\beta = 0.1$, $e = 0.05$, $b = -1$, $\tau_{1,Y} = 1$, $\kappa_1 = 1$, $m_1 = 1$, $\tau_{2,Y} = 0.8$, $\kappa_2 = 0.8$.